Spin-polarized electroluminescence and spin-dependent photocurrent in hybrid semiconductor/ferromagnetic heterostructures: An asymmetric problem

P. Renucci,[1] V. G. Truong,[1] H. Jaffrès,[2] L. Lombez,[1] P. H. Binh,[3] T. Amand,[1] J. M. George,[2] and X. Marie[1]
[1], *Université de Toulouse, INSA-CNRS-UPS, LPCNO,135 Avenue de Rangueil, F-31077 Toulouse, France*
[2]*Unité Mixte de Physique CNRS/Thales Campus de Polytechnique, 1 Avenue A. Fresnel, 91767 Palaiseau Cedex, France and Université Paris-Sud 11, 91405 Orsay, France*
[3]*Institute of Material Science, 18 Hoang Quoc Viet Road, Cau Giay District, Hanoï, Vietnam*
(Received 16 July 2010; published 15 November 2010)

We have measured in the same hybrid semiconductor/ferromagnetic (FM) metal structures the photocurrent obtained under polarized optical excitation and the polarized electroluminescence recorded under forward electric bias (spin light-emitting diode operation). The systematic investigations have been performed on devices with different ferromagnetic spin injectors: tunnel barrier of Al_2O_3 surmounted by a thin Co ferromagnetic layer or MgO tunnel barriers with a CoFeB FM layer. The semiconductor part of the device is composed of an AlGaAs diode with a GaAs/AlGaAs quantum well embedded in the intrinsic region. Though a very efficient electrical spin injection is demonstrated with a measured circular polarization of the electroluminescence up to 30% for an external field of 0.8 T, very weak polarizations of the photocurrent are evidenced whatever the nature of the device is. The maximum photocurrent polarization obtained under continuous resonant circularly polarized excitation of the quantum well excitons is about 3%. This demonstrates that the investigated devices do not act as an efficient spin filter for the electrons flowing from the semiconductor part toward the ferromagnetic part of these structures though these layers are very efficient spin aligners for electrical spin injection. We interpret the weak measured polarization of the photocurrent in the percent range as a consequence of the Zeeman splitting of the quantum well excitons which yields different absorption coefficients for the polarized excitation laser with different helicities. This leads to different intensities of photocurrent collected for the two different circularly polarized excitations. This interpretation is confirmed by an experiment exhibiting the same results for photocurrent measured on a device with a nonferromagnetic electrode.

DOI: 10.1103/PhysRevB.82.195317 PACS number(s): 75.76.+j, 85.75.−d, 78.60.Fi, 78.67.De

I. INTRODUCTION

The electrical injection of spin-polarized currents from magnetic metals into semiconductors has been widely explored for about 10 years.[1,2] An elegant way to demonstrate an electrical spin injection is to measure optically the polarization of the electroluminescence in the so-called spin light-emitting diode (spin-LED) devices.[3–6] Most of the studies have been devoted to systems involving Schottky or insulator tunnel barriers between the ferromagnetic metal and the semiconductor.[7–9] Polarizations of the electroluminescence up to 52% have been evidenced in these structures, demonstrating unambiguously the efficiency of electrical spin injection even at room temperature.[10]

The symmetrical challenge which consists in an electrical detection of a spin-polarized current of carriers is also a requirement for future spintronic devices. Some spectacular experiments have been realized with coupled electrical and optical techniques as in Refs. 11 and 12 where spin imaging is obtained through spatially resolved Kerr rotation or full electrical measurements. In a similar vein, more recent works have demonstrated the possibility to convert the light polarization into an electrical signal through inverse spin-Hall-effect-like experiments.[13,14] On the other hand, large efforts to provide a voltage detection[15–21] of the spin accumulation electrically generated in a semiconductor has been initiated in the so-called nonlocal[16–18] geometry as well as in the two-point[20] and three-point geometries;[15,19,21] the latter method being favorably employed to probe spin accumulation just beneath the tunnel spin injector.

An alternative way to probe the ability of the ferromagnetic (FM) layer to act as a spin filter is (i) to pump a well controlled spin-polarized electron density in the semiconductor by optical orientation[22] with circularly polarized light and (ii) to detect the photocurrent through the interface in a vertical transport geometry.[23–31] The photocurrent polarization is obtained through a modulation of the helicity of the excitation light for a fixed external magnetic field *or* equivalently through a reversal of the magnetic field orientation with a fixed helicity of the excitation light. In contrast to the investigation of electrical spin injection in spin-LEDs, just a few experimental works using this technique have been reported. Taniyama *et al.*[28] have evidenced a photocurrent polarization of 1.7% at 300 K for an external field $B\sim 2$ T for a $GaAs/AlO_x/Fe$ interface. Isakovic *et al.*[26,30] estimated a polarization of about 0.5% for $B\sim 2$ T due to spin-dependent transport under an excitation above the GaAs band gap in ferromagnetic-GaAs Schottky diodes with InGaAs quantum wells at $T=10$ K. The same authors demonstrated the key role played by background effects [magnetic circular dichroism (MCD) in the FM layer and Zeeman effects in the semiconductor] on the measured photocurrent. All these experimental investigations yield very weak measured photocurrent polarization, i.e., never exceeding a few percents. This contrasts with the very large circular polarization of the electroluminescence which is obtained under forward

bias of this kind of devices, i.e., in the spin-LED operation. Jonker and co-workers reported, for instance, electroluminescence circular polarization up to 32% in a Fe/AlGaAs/GaAs spin-LED device with a Schottky barrier[6] in the tunneling transport regime, a structure that present some similarities with the ones investigated in photocurrent measurements.[25,26] However, a direct and clear comparison remains difficult in general since the measurements are usually performed on different devices and at different temperatures.

In order to get further insights on this problem, we present in this paper a systematic investigation of both polarized photocurrent and polarized electroluminescence measurements in a series of hybrid FM/semiconductor structures. For increasing the generality of our results we have tested two kinds of interfaces that involve tunnel oxide barriers which are commonly used in electrical spin-injection devices,[6,10,32] i.e., MgO/CoFeB and Al_2O_3/Co. We also studied devices with different quantum well barrier heights (aluminum content 8% or 15% for the AlGaAs barrier) to probe its role on the polarized photocurrent. Our experiments are carried out in a wide range of temperatures ranging from low temperature (20 K) up to 160 K.

From all these measurements we conclude that the devices based on FM spin aligners providing very efficient electrical spin injection in the semiconductor can hardly act as efficient spin filters in spin photocurrent experiments in continuous wave (cw) regime. For all the investigated devices we measure a maximum photocurrent polarization of about 3% and we demonstrate that this effect does not originate from an expected spin-filtering effect but from a different absorption of the polarized excitation light due to the Zeeman splitting of the exciton in the GaAs quantum well (QW). We show that these structures, optimized for electrical spin injection, are not suitable to evidence spin photocurrent phenomena under cw excitation.

The paper is organized as follows. Section II describes the hybrid semiconductor/metal devices which are studied by several complementary techniques. The different setups of photocurrent, electroluminescence (EL), and time-resolved photoluminescence (TRPL) are also presented. The experimental results of photocurrent spectroscopy showing very weak polarizations ($\leq 3\%$) are presented in Sec. III. In contrast efficient electrical injection under forward bias of spin-polarized electrons is measured by polarization-resolved electroluminescence in the same devices (Sec. IV). In order to interpret the results, complementary TRPL measurements are also performed for various temperatures. These TRPL measurements provide an independent characterization of the spin dynamics in the quantum well and its temperature dependence. A discussion of the results enlightening the fundamental differences in the two operation modes of the device is finally presented in Sec. V.

II. SAMPLES AND EXPERIMENTAL SETUPS

The studied samples are hybrid semiconductor/metal structures [Fig. 1(a)] that were grown by molecular-beam epitaxy for the semiconductor part and by sputtering for the tunnel barrier/ferromagnetic metal part. We have fabricated

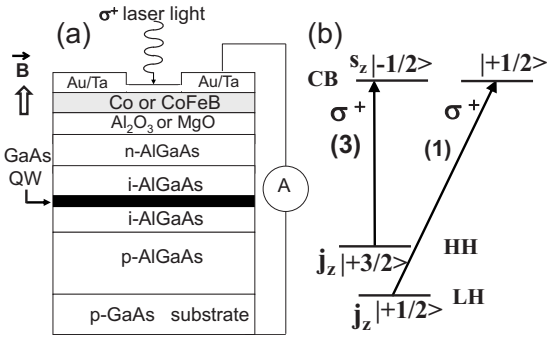

FIG. 1. (a) Photocurrent measurement principle on a hybrid semiconductor/ferromagnetic layer device with a GaAs/AlGaAs quantum well embedded in the intrinsic region. (b) Optical selection rules in a GaAs quantum well for a circularly polarized excitation σ^+. Oscillator strengths for each transition are in brackets.

and tested a large set of samples. We present here the results on five of them which reflect the general behavior.

The semiconductor part of the samples consists in a *p-i-n* $Al_xGa_{1-x}As$ structure grown on a *p*-doped GaAs:Zn substrate ($p=4\times10^{17}$ cm^{-3}). The *p*-doped $Al_xGa_{1-x}As$:Be layer ($p=1.4\times10^{19}$ cm^{-3}) is 500 nm thick. The doping of the *n*-$Al_xGa_{1-x}As$ layer (thickness: 50 nm) is 10^{16} cm^{-3} to minimize the spin-relaxation processes.[33] The intrinsic $Al_xGa_{1-x}As$ zone contains a 10 nm symmetric GaAs quantum well (with $Al_xGa_{1-x}As$ barriers of 50 nm). The structure was capped by amorphous As. The sample is then transferred from the molecular beam epitaxy machine in the atmosphere to a separated chamber. It was desorbed at 450 °C under ultrahigh vacuum in this chamber in which desorption is monitored by reflection high-energy electron diffraction. For samples AS1, AS2, and B1, the Al content in the barrier is 8%. In order to investigate the effect of the barrier height, sample B2 is fabricated with an Al content of 15%.

The samples were then transferred *in situ* in the sputtering chamber where tunnel insulator and ferromagnetic thin films were grown. For sample AS1, the top contact is composed of an Al_2O_3 tunnel barrier (2.2 nm) and a cobalt ferromagnetic thin film (8 nm) grown at room temperature. The tunnel barrier was formed by oxidation of 1.5 nm Al under a O_2 and Ar plasma. Gold cap layer (2 nm) was finally deposited to prevent cobalt from oxidation. The size of the contact area on the sample is 3×3 mm^2. AS2 is a test structure without Al_2O_3 and Co for time and polarization-resolved photoluminescence experiments.

For samples B1 and B2, the top contact is composed of a MgO tunnel barrier and a CoFeB ferromagnetic layer.[34] The MgO barrier has a thickness of 2.6 nm grown at 300 °C, followed by a 3 nm $Co_{40}Fe_{40}B_{20}$ FM contact capped with 5 nm Ta layer to prevent oxidation. The sputtering conditions for MgO and metals can be found elsewhere.[34] Finally sample C is a test sample where the FM contact is replaced by a simple non-FM platinum (Pt) layer with a thickness of 3 nm. The samples characteristics are summarized in Table I. Circular mesas with 300 μm diameter were then processed using standard photolithography and etching techniques.

The photocurrent measurements are performed at normal incidence under an optical excitation provided by a cw cir-

TABLE I. Samples characteristics.

Sample name	Al in AlGaAs/GaAs QW (%)	Tunnel barrier	Metal
AS1	8	Al_2O_3	Co
AS2	8	No	No
B1	8	MgO	CoFeB
B2	15	MgO	CoFeB
C	8	MgO	Pt

cularly polarized Ti-sapphire laser with a tunable wavelength. The intensity of the laser is monitored by a silicon photodiode. The incident power is about 15 mW and the laser is focused on a spot with a 100-μm-diameter size (we have checked that the measured photocurrent signal is linear with the incident laser power). The circular polarization of the laser excitation ($\sigma+$ or $\sigma-$) is tuned using electrically controlled liquid-crystal retardation plates. The photocurrent intensities J_+ and J_- generated, respectively, by circularly right ($\sigma+$) and left ($\sigma-$) polarized light are detected through the voltage variation measured on a load resistor of 500 Ω. The circular polarization P_c^J of the photocurrent is defined as $P_c^J=\frac{(J_+-J_-)}{(J_++J_-)}$.[35] All the photocurrent experiments are realized under a magnetic field produced by a Helmoltz coils (0–0.8 T) in a closed-cycle cryostat with a temperature ranging from 20 to 300 K. For the EL measurement, the device was placed in the same cryostat and forward biased with squared shape voltage pulses of 1 μs width and a repetition rate of 50 kHz. The EL signal was detected in the Faraday geometry (applied magnetic field along the growth axis) by a standard setup (monochromator equipped by a cooled low noise charge coupled device camera) with a spectral resolution of about 2 meV. For TRPL experiments, a mode-locked Ti:sapphire laser (1.5 ps pulse width) was used for the nonresonant circularly polarized excitation at ~1.697 eV (i.e., in the AlGaAs barrier). The PL signal was detected by a synchroscan streak camera, which provides an overall temporal resolution of 8 ps. The circular polarization P_c of the luminescence is defined by the following quantity $P_c^L=\frac{(I_+-I_-)}{(I_++I_-)}$. where I_+ and I_- are relative, respectively, to the right and left circularly polarized components of luminescence. P_c^L is analyzed by passing EL and PL through a $\lambda/4$ wave plate and a linear analyzer. Finally we will refer in the following to forward and reverse biases applied to the devices, keeping in mind these terms are relative to the bias across the *p-i-n* junction. Thus, a forward bias corresponds to a positive voltage applied to the *p* substrate of the device with respect to the top metallic electrode.

III. PHOTOCURRENT MEASUREMENTS

We present first the photocurrent measurements performed at 20 K under circularly polarized light at zero bias ($V_{bias}=0$) in sample AS1. The experiments are carried out under an excitation laser with photon energies resonant with the exciton absorption lines of the GaAs/AlGaAs quantum well (when the laser is tuned with the heavy exciton line, an initial 100% spin-polarized electrons population can be generated due to optical selection rules[22]). The photogenerated excitons are dissociated by the internal electric field inside the *p-i-n* junction: electrons extracted by tunnel effect from the quantum well flow into the *n*-AlGaAs layer and through the insulator Al_2O_3 tunnel layer, before passing through the ferromagnetic Co layer. Figure 2(a) displays the measured photocurrent $J=J_++J_-$ as a function of the laser excitation energy with and without longitudinal magnetic field (0.8 T) for sample AS1. One can see a clear signature of the heavy-hole exciton (XH) and light-hole exciton (XL) lines. The splitting between these two lines is of about 7.5 meV, which is consistent with an aluminum concentration of 8% for a GaAs/AlGaAs 10 nm quantum well. As expected the weak external field of 0.8 T does not change significantly the photocurrent spectrum. We turn now to the dependence of the photocurrent polarization P_c^J with the laser excitation energy [Fig. 2(b)]. When $B=0$, the current polarization remains below ≈0.3%. For $B=0.8$ T, a clear oscillation of the polarization is evidenced: a peak of positive polarization of about 2.7% appears at $E_{max}=1.545$ eV followed by a dip of negative polarization at $E_{min}=1.548$ eV. For a magnetic field of 0.8 T, and a Co layer of 8 nm, the background effect associated to the magnetic circular dichroism of the FM layer that may contribute to the photocurrent polarization can be ruled out: we have checked that this contribution is smaller than 0.4% by measuring the photocurrent polarization under linearly polarized excitation light (not shown). We note in Fig. 2(b) that the positive peak of photocurrent polarization does not coincide with the XH line but is rather situated close to the XL absorption peak.

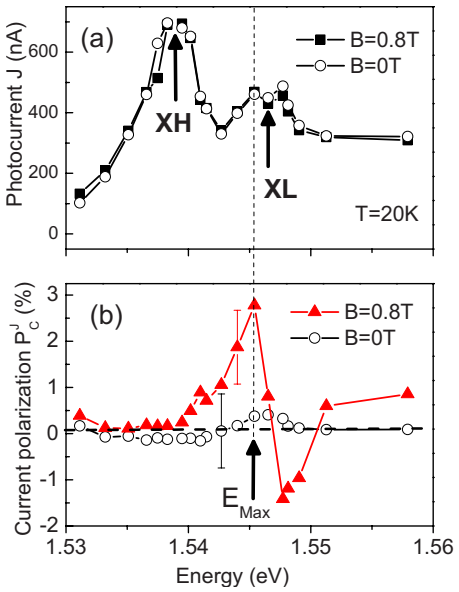

FIG. 2. (Color online) Sample AS1; $V_{bias}=0$. (a) Photocurrent spectra for $B=0$ (opened circles) and $B=0.8$ T (bold squared). (b) Polarization of the photocurrent as a function of the laser energy for $B=0$ T (opened circles) and $B=0.8$ T (bold triangles). The vertical dashed line is a guide for the eyes.

In Fig. 3(a), the amplitude of the photocurrent polarization peak (detected for E_{max}) is plotted as a function of the

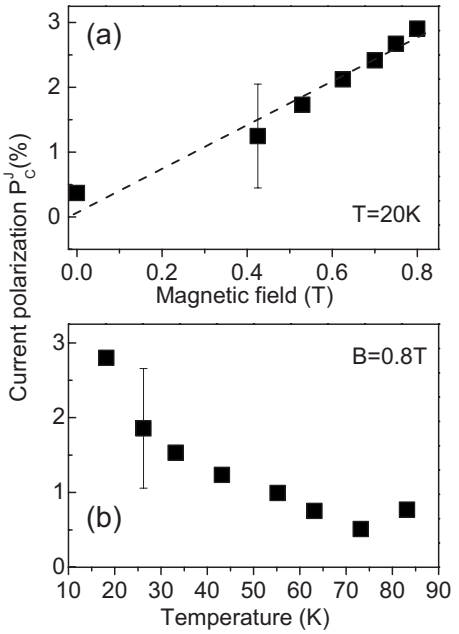

FIG. 3. Sample AS1; V_{bias}=0. (a) Photocurrent polarization (measured at E_{max}) as a function of the longitudinal magnetic field. The dashed line is a guide for the eyes. (b) Polarization (measured at E_{max}) of the photocurrent as a function of temperature for a magnetic field B=0.8 T.

applied magnetic field. Let us emphasize here that the applied magnetic field is not sufficient to saturate the magnetization of the thin Co layer along the growth axis of the structure but only has the effect to rotate the magnetization from the in-plane to the out-of-plane direction. The behavior of the current polarization could be consistent with the increase in the component along the growth axis of the magnetization of the Co layer in the range of magnetic fields explored. As in Ref. 28, these results could thus be interpreted in terms of efficient spin-filtering effect of the FM layer. We will show in the following that it is definitely not the case.

All the previous measurements were performed at 20 K. We investigate now the influence of the temperature on the measured photocurrent polarization. Figure 3(b) displays the decreasing behavior of P_c^J (measured again at E_{max}) with temperature under B=0.8 T. Note that E_{max} follows the same behavior with temperature as the energy band gap of GaAs. P_c^J exhibits a decreasing trend with temperature.

We have also performed the same investigations in hybrid FM/semiconductor structures where the Al_2O_3/Co layers are replaced by a MgO/CoFeB layers which are known to yield very high electrical spin-injection efficiencies.[10,32] Figure 4 displays the photocurrent characteristics (intensity and polarization) as a function of the excitation light energy in sample B1 at T=20 K (AlGaAs barrier with 8% of aluminum content, i.e., the semiconductor part of the structure is identical to samples AS1). The results are very similar to the ones obtained in sample AS1 [Fig. 2(b)], displaying the same oscillating behavior close to the XL line. A polarization close to zero is again measured on the low-energy side of the XH absorption and a maximum of polarization of about 3% is

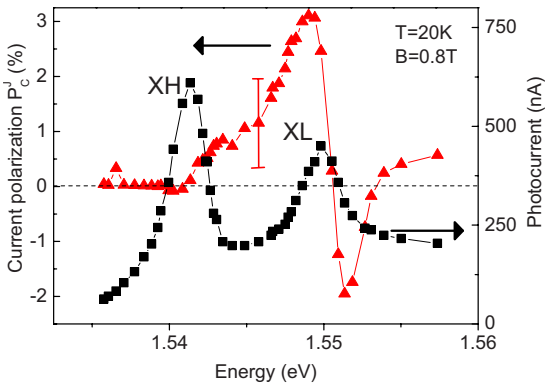

FIG. 4. (Color online) Sample B1; V_{bias}=0. Left axis: polarization of the photocurrent as a function of the laser energy (bold triangles). Right axis: photocurrent spectrum (bold squared).

measured in the vicinity of the XL absorption. The same trend is observed at higher temperature (160 K) for AlGaAs barriers with 15% aluminum content (not shown).

Moreover, we have investigated the role of the band profile away from zero bias on the measured photocurrent polarization. By applying a reverse bias we could expect a more efficient extraction efficiency of the carriers from the quantum well. However, under an external bias of V_{bias}= −0.8 V and T=160 K on sample B2, a polarization close to zero is again measured on the low-energy side of the XH absorption line and a maximum polarization of about 1.5% is evidenced close to the XL line (Fig. 5). This demonstrates that the negative external bias has a weak effect on the small polarized photocurrent measured in these devices. The latter could be explained by the fact that the spin-polarized electrons are photogenerated in the quantum well and lose their spin orientation before reaching the ferromagnetic layer (i.e., during the extraction process from the QW) in the range of negative bias explored. To reduce this effect we have also measured the polarized photocurrent following a laser excitation in the AlGaAs barrier (spin-polarized electrons do not need anymore to be extracted out of the well by tunnel effect). However, almost no photocurrent polarization was observed in these conditions.

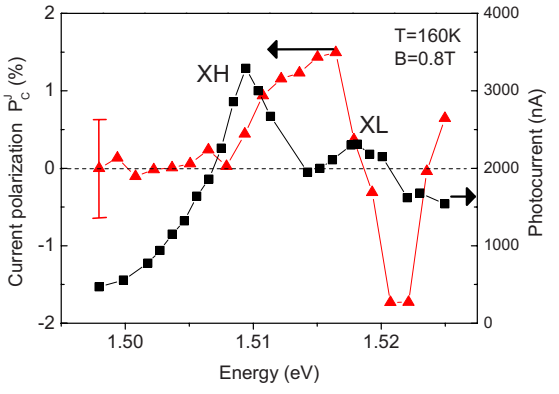

FIG. 5. (Color online) Sample B2; V_{bias}=−0.8 V. Left axis: polarization of the photocurrent as a function of the laser energy (bold triangles). Right axis: photocurrent spectrum (bold squared).

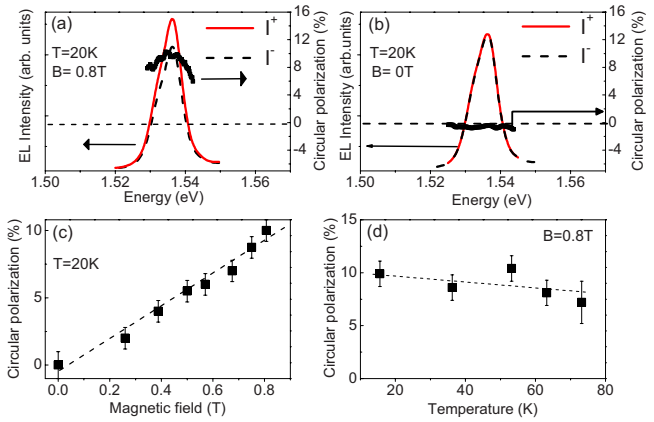

FIG. 6. (Color online) Sample AS1. Spin-LED operation. V_{bias} =4.7 V; current: 600 mA (current density: 6.5 A cm^2). (a) B =0.8 T. Left axis: I^+ (solid line) and I^- (dashed line) components of EL. Right axis: corresponding circular polarization rate of the electroluminescence (bold squared). (b) B=0 T. Left axis: I^+ (solid line) and I^- (dashed line) components of EL. Right axis: corresponding circular polarization rate of the electroluminescence (bold squared). (c) Circular polarization rate of EL as a function of magnetic field. The dashed line is a guide for the eyes. (d) Circular polarization rate of EL as a function of temperature for B=0.8 T. The dashed line is a guide for the eyes.

IV. ELECTRICAL SPIN-INJECTION MEASUREMENTS

In order to get further insights on the investigated hybrid structures, we have then performed polarization-resolved electroluminescence experiments in the same devices studied in Sec. II, now operated as conventional LEDs by applying a forward bias (with respect to the *p-i-n* junction) to the structures.[1,2,4–6,10,32] Results on the polarization of the emitted light are displayed in Fig. 6 for sample AS1. When B =0, both circularly polarized components of the electroluminescence related to the XH line are superimposed [Fig. 6(b)], corresponding to a zero circular polarization rate as it is expected. On the contrary, when a longitudinal magnetic field of 0.8 T is applied [Fig. 6(a)] rotating the magnetization in the out-of-plane direction, an electroluminescence circular polarization P_c^L of about 10% is measured. Figure 6(c) shows the dependence of this circular polarization rate as a function of the applied magnetic field. It is consistent with the increase in the projection of the magnetization of the Co layer along the growth axis, that is the quantization axis, in the range of magnetic fields explored. As the hole spin is not polarized under electrical excitation, the circular polarization of the luminescence P_c measured for the XH exciton line reflects directly the electron spin polarization $P_e=\frac{(n_+-n_-)}{(n_++n_-)}$ (where n_+ and n_- are relative to the populations of electrons with spin $S_z=+1/2$ and $S_z=-1/2$, respectively). As the electron spin can undergo spin relaxation within the quantum well during its lifetime, P_c is a low limit for P_e in a cw experiment. A factor of merit $\eta=P_c^L/P_{Co}$ of the spin injection can be estimated. For a magnetic field of 0.8 T, the electron spin polarization P_{Co} in the Co (at the Fermi level), which tracks the magnetization of the Co layer, is of about 18% ($P_{Co}\approx 42\%$ for B=1.7 T, at saturation[36]). This leads to a

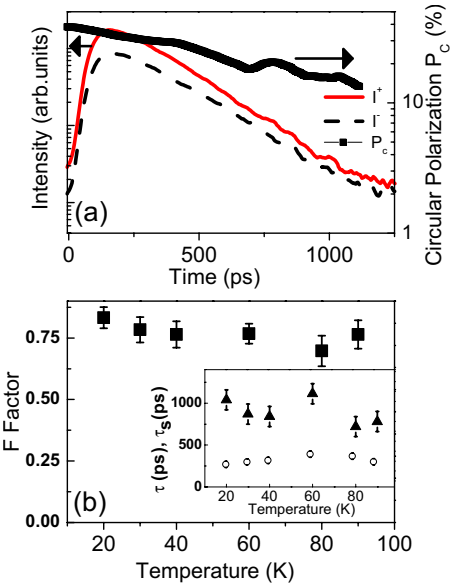

FIG. 7. (Color online) Sample AS2. (a) Left axis: copolarized and counterpolarized luminescence intensity components (I^+ and I^-, respectively) as a function of time following a picosecond σ+ polarized excitation laser pulse. Right axis: corresponding time-resolved circular polarization rate P_c (bold squared); logarithmic scale. (b) Evolution of the F factor with temperature. Insert: evolution of the measured electron-spin relaxation time τ_s (bold triangles) and electron lifetime τ (open circles) with temperature.

factor of merit of about 50% at 20 K. It is comparable to the results obtained by Jonker and co-workers for a Fe/Al_2O_3 spin injector[6] and demonstrates the quality of our device as an efficient spin-polarized electron injector. We can notice the much larger polarization measured here for electrical spin injection compared to the very weak polarization of the photocurrent extracted from the same sample (see Sec. II). To complete these measurements, we have also probed the evolution of the circular polarization of the electroluminescence with temperature. Figure 6(d) exhibits a relative stability of this circular polarization up to 70 K, with a slight decreasing trend.

In order to interpret the photocurrent and electroluminescence experiments at various temperatures, the electron spin-relaxation time in the quantum well is an important parameter of the problem and should be measured independently. This explains why we have performed time and polarization resolved photoluminescence experiments[22] on sample AS2, similar to sample AS1, but without Al_2O_3 and cobalt layers. The laser excitation is tuned above the band gap of the AlGaAs barrier ($h\nu\sim 1.697$ eV). Under these nonresonant excitation conditions, the hole spin-relaxation time is very short[37] and the circular polarization of the luminescence measured for the XH exciton line reflects then directly the electron spin polarization. Figure 7(a) displays the copolarized and counterpolarized PL intensity components, I^+ and I^-, versus time at 20 K and the corresponding circular polarization dynamics P_c^L. We find an electron spin-relaxation time of $\tau_s\sim 1000$ ps and a carrier lifetime $\tau\sim 250$ ps at T =20 K. The temperature dependence of the electron spin-relaxation time is displayed in the inset of Fig. 7(b) up to 90

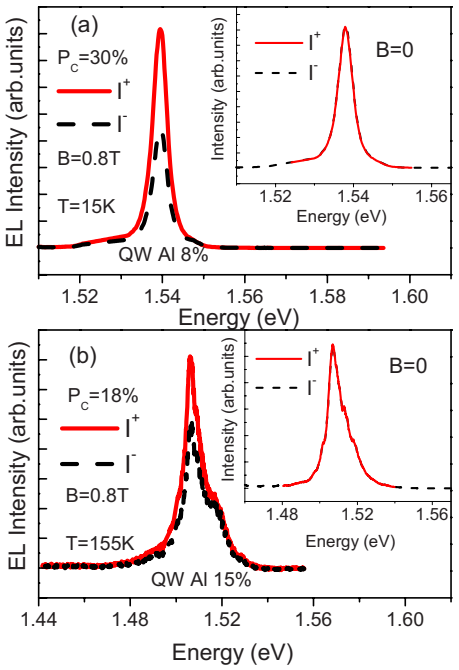

FIG. 8. (Color online) (a) Sample B1. Spin-LED operation. $V_{bias}=2.45$ V; current: 10 mA (current density: 14 A cm^2). $B=0.8$ T. I^+ (solid line) and I^- (dashed line) components of EL. Inset: same quantities for $B=0$ T. (b) Sample B2. Spin-LED operation. $V_{bias}=1.85$ V; current: 12 mA (current density: 17 A cm^2). $B=0.8$ T. I^+ (red line) and I^- (black line) components of EL. Inset: same quantities for $B=0$ T.

K. No strong dependence is observed in this temperature range.

Using these complementary results obtained by TRPL, we can now interpret the behavior of the circular polarization of the electroluminescence with temperature displayed in Fig. 6(d) for sample AS1. One has to consider that, under cw electrical excitation, the circular polarization rate of electroluminescence is related to the circular polarization of electrons $P_e^{initial}$ just before they are trapped in the quantum well by $P_c=FP_e^{initial}$. The F factor can be written as $F=\frac{1}{1+\frac{\tau}{\tau_s}}$, where τ and τ_s are, respectively, the luminescence lifetime and the electron spin-relaxation time.[38,39]

As it can be seen in the inset of Fig. 7(b) (bold triangles), τ_s is larger than 700 ps in the range of temperatures explored. Besides the electron spin-relaxation time τ_s, the lifetime τ can also be measured; we find $\tau\sim 250-350$ ps in the investigated temperature range [inset of Fig. 7(b); open circles]. It allows us to calculate the F factor [Fig. 7(b)]. As τ_s is larger than τ, F remains close to the value 0.75. So one can deduce from the relative stability of the circular polarization of the electroluminescence with temperature on the one hand and of the constant value of the F factor around 0.75 on the other hand, that the electrical spin-injection process through the interface is efficient and stable up to 70 K. Let us recall that the photocurrent polarization measured on the same sample in the same temperature range is in contrast very weak [about 2.7% at $T=20$ K and ~ 0.5 % at $T=70$ K, see Fig. 3(b)].

The same striking difference is observed for samples B1 and B2 where the Al_2O_3/Co layers are replaced by MgO/CoFeB layers. Figure 8(a) presents the characteristics of the polarized electroluminescence of sample B1 at $T=20$ K. We measure a circular polarization of 30% at $B=0.8$ T, demonstrating the very efficient electrical spin injection in this spin-LED device. Again this polarization is much larger than the one measured in photocurrent spectroscopy (about 3%, see Fig. 4). For higher temperature the electrical spin injection is still robust as shown in Fig. 8(b) where the electroluminescence circular polarization is close to 18% at $T=160$ K in sample B2. Note that it is possible to measure the EL intensity at $T=160$ K (and even at room temperature) in sample B2 contrary to sample AS1 because of the higher AlGaAs barrier (15% Al) in the former that allows a better carrier confinement. Nevertheless the photocurrent polarization measured on the same device is again very weak [see Fig. 5(a)].

In summary all the FM/semiconductor hybrid structures investigated here exhibit large EL circular polarization, demonstrating efficient electrical spin injection. However, in the reverse operation regime, i.e., polarized photocurrent under cw laser excitation, very small polarizations are measured that we discuss in more details in the next paragraph.

V. DISCUSSION

First we propose to comment on the excitation energy dependence of the polarized photocurrent measurements [Figs. 2(b), 4, and 5 in samples AS1, B1, and B2, respectively). As demonstrated below these measurements are key elements to interpret the spin physics of these hybrid FM/semiconductor structures. To simplify the interpretation we have first measured the variation in the carrier spin polarization as a function of the excitation energy in a structure (AS2) with no FM layer (photoluminescence under circularly polarized light σ^+). This measurement gives a good picture of the dependence of the photogenerated carriers spin polarization as a function of the laser excitation energy.[40,41] We then compare this dependence with the one measured by photocurrent in the hybrid structure.

Let us recall the well-known optical selection rules for optical orientation experiments in a GaAs/AlGaAs quantum well.[22] Due to confinement, the degeneracy between heavy-hole (HH) and light-hole (LH) levels is lifted in the center of the Brillouin zone. The transfer of the angular momentum of a circularly polarized photon will result in two different bound electrons-hole pairs involving different electrons spin depending on the nature of the optical transition. A photon [see Fig. 1(b)] from circularly right polarized light will create a $(S_z:|-\frac{1}{2}\rangle;J_z:|+\frac{3}{2}\rangle)$ electron-hole pair if the laser is tuned on the E-HH transition whereas it will create in addition $(S_z:|+\frac{1}{2}\rangle;J_z:|+\frac{1}{2}\rangle)$ electron-hole pair if the laser is tuned on the E-LH transition (with an oscillator strength three time smaller). Here S_z and J_z are the projections along the growth axis of the total angular momentum of the electron and the hole, respectively.

The dependence of the photogenerated carrier spin polarization as a function of the laser excitation energy $h\nu$ can be easily measured independently in a polarized excitation of photoluminescence (PLE) experiment.[40,41] We have per-

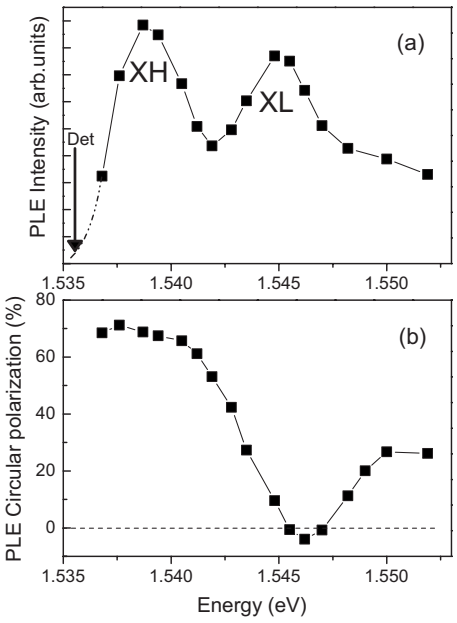

FIG. 9. Sample AS2 (a) PLE intensity (i.e., XH photoluminescence intensity as a function of the laser excitation energy $h\nu$) measured at $T=15$ K. The vertical arrow indicates the detection energy which corresponds to the XH emission peak. (b) Circular polarization of the XH photoluminescence as a function of the laser excitation energy $h\nu$. The cw excitation laser light is circularly polarized σ^+.

formed this experiment on the test sample AS2 which is identical to the other samples except that there is no FM layer. Figure 9(a) displays the PLE intensity measured at $T=15$ K where the two excitons absorptions lines (at E_{XH} for XH and E_{XL} for XL) are clearly evidenced. The detection energy is set to the XH PL emission energy. In Fig. 9(b) the circular polarization of the XH photoluminescence is presented as a function of the laser excitation energy $h\nu$. When $h\nu \approx E_{XH}$, we measure a very large PLE circular polarization, up to 70% (reflecting the photogenerated electron-spin polarization). For larger photon energies $h\nu$, the circular polarization drops, becomes negative when $h\nu=E_{XL}$ and finally increases up to 20%. This behavior is exactly what we expect in a quantum well due to the optical selection rules.[40,41] The negative value observed when the laser energy is resonant with the XL is due to the larger oscillator strength of the XL exciton compared to the one of the E-HH pair transition occurring at the same energy.

At this stage let us mention two important features when one compares the polarized PLE and the polarized photocurrent experiments [Figs. 2(b) and 9(b), for instance): (i) a very large electrons spin polarization is photogenerated when $h\nu \approx E_{XH}$ while zero spin-polarized photocurrent is measured for the same energy: for instance, at $h\nu=1.537$ eV, the photogenerated electron spin polarization is 70% [Fig. 9(b)] and the polarized photocurrent polarization is P_c^J about 0 ($\pm 0.2\%$). No spin photocurrent is thus measured though a strong electron spin polarization is photogenerated.

(ii) A small negative circular polarization is observed in both experiments for excitation energies close to the XL absorption at $h\nu=1.546$ eV. A fast interpretation of the data for these excitation energies would then lead to the conclusion that the FM layer in that case would act as a spin filter and a spin photocurrent would be evidenced. Nevertheless, we demonstrate below that this interpretation is not valid.

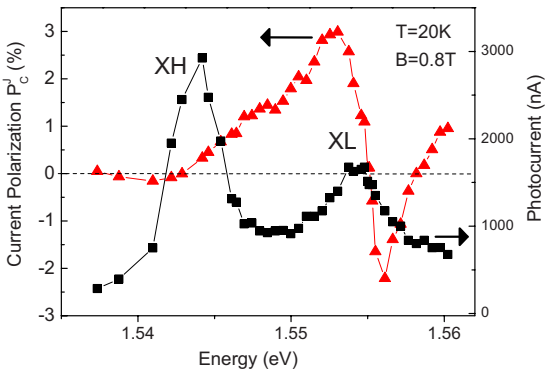

FIG. 10. (Color online) Sample C. $V_{bias}=0$. Left axis: polarization of the photocurrent as a function of the laser energy (bold triangles). Right axis: photocurrent spectrum (bold squared).

As the results look rather contradictory (apparent observation of spin photocurrent for $h\nu \sim E_{XL}$ and no spin photocurrent for $h\nu \sim E_{XH}$ though the photogenerated electron spin polarization is much larger), we have measured the polarized photocurrent on a test sample where the FM layer has been replaced by a nonmagnetic platinum layer (sample C).

Figure 10 displays the photocurrent characteristics (intensity and polarization) as a function of the excitation light energy in sample C at $T=20$ K. The surprising result is that the data are very similar to the ones obtained in samples AS1, B1, and B2 where FM layers were expected to play a spin-filtering effect. No polarization is measured for $h\nu \sim E_{XH}$ and the maximum polarization, measured in the vicinity of the XL absorption, is on the order of 2.9%. The same oscillating behavior (a positive peak followed by a negative one) is observed. The conclusion is that no spin photocurrent originating from filtering effects has been evidenced in our experiments whatever the nature of the hybrid structure (samples AS1, B1, and B2).

The observation of a small polarized photocurrent signal for excitation energies close to XL more likely originates from the following background Zeeman splitting effect. The exciton Zeeman splitting in the external 0.8 T field yields a slightly different absorption coefficient for $\sigma+$ or $\sigma-$ excitation light. As a consequence, the photocurrent intensity is different for $\sigma+$ or $\sigma-$ excitation yielding a polarized photocurrent signal with an oscillating behavior close to the exciton absorption. Why do we observe this effect on the light-hole exciton and not on the heavy-hole exciton? It is simply due to the very different exciton g factor for XH and XL.[42–44] Carmel *et al.* measured a longitudinal exciton g factor for XL five times larger than the XH one;[44] this was confirmed by magnetophotoluminescence experiments performed by Chen *et al.* who claimed a factor 8 difference.[42] This explains that for our modest external magnetic field of 0.8 T, no polarization is measured in the XH region whereas a value on the order of 2–3 % is detected when the laser is resonant with the XL absorption line. Figure 11 confirms this interpretation. We have performed a very simple simulation

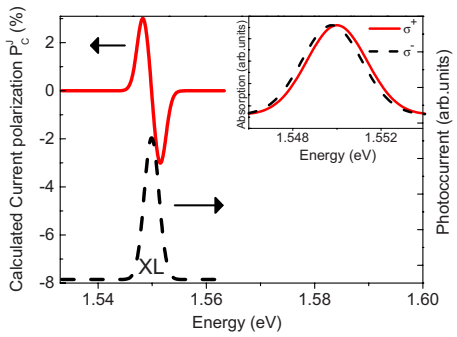

FIG. 11. (Color online) Simulation. Left axis: current polarization as a function of the laser energy for $B=0.8$ T. Right axis: photocurrent intensity as a function of the laser energy for $B=0$. Inset: absorption (a.u.) as a function of the laser energy for $B=0.8$ T for σ^+ (solid line) and σ^- (dashed line) polarized light. For these simulations, XL linewidth=3.2 meV (sample B1) and XL g factor=5.

of the photocurrent measurement by considering two Gaussian XL exciton absorption lines separated by the Zeeman splitting corresponding to 0.8 T. Using the light-hole exciton g factor ($\approx$5) measured in Ref. 42, a linewidth (of 3.2 meV) and a relative oscillator strength of the XL absorption with respect to the E-HH free-carrier absorption extracted from measurements of Fig. 4, we reproduce quite fairly the experimental results of Fig. 4: a polarized signal of about 3% with a positive and negative oscillation is observed in the vicinity of the XL absorption line. This demonstrates that the FM layers play no spin-filtering effects in the photocurrent measurements presented in this paper: the weak polarization ($\leq$3%) evidenced in the experiments is simply attributed to the Zeeman splitting of the XL absorption. Note that the decreasing value of the photocurrent polarization with temperature displayed in Fig. 3(b) for AS1 could be explained by the broadening of the XL line with temperature.

Let us now come back to previous published results. Polarized photocurrent measurements in hybrid $Ni_{80}Fe_{20}$/GaAs Schottky diode structures were previously reported by Hirohata *et al.*[45] The excitation light was absorbed in bulk GaAs and the variation in the photocurrent upon the light helicity was measured. These authors initially claimed the observation of spin-dependent transport due to spin filtering in this structure but more recently the same group performed systematic investigation with different FM layers (NiFe, Co, and Fe) and concluded that at reverse and zero bias only circular dichroism ($<$0.6%) was found and no spin-filtering effect could be evidenced.[31] This is in agreement with our results obtained with the aforementioned hybrid FM/semiconductor structures with insulator tunnel barriers (Al_2O_3 or MgO). The key point in our measurements is that we have checked on the same structure that the FM layer acts as an efficient spin aligner for electrical spin injection (spin-LED operation) *whereas the efficiency of this spin aligner was not probed in previous published works*.

Moreover, we now may provide further comments about the very interesting work on spin photocurrent that was also performed by Isakovic *et al.*[26,30] in a device composed of an InGaAs/GaAs quantum well and a Fe (or FeCo) FM layer on a Schottky diode structure. They measured weak polarized photocurrent signals (on the order of a few percents). Nevertheless considering the importance of background effects (MCD in the FM layer and Zeeman effects in the semiconductor), they considered their results as suggestive of spin transport but not conclusive. Our results obtained on devices with insulating tunnel barriers confirm that the background effects explain the weak measured polarized photocurrent.

The fundamental question is why spin-filtering effects of the FM *layer can hardly be evidenced in these photocurrent measurements though the same devices, as demonstrated in this paper, exhibit strong electrical spin-injection efficiencies*. As initially suggested by Isakovic *et al.*,[30] the key point to measure spin photocurrent induced by spin-filtering effects of the FM layer is that the minority photogenerated electrons (that is to say with a spin aligned in the direction opposite to the magnetization of the magnetic layer) which are reflected by the FM layer must undergo efficient recombination (for example, with holes) in the semiconductor; otherwise they could simply bounce back and finally enter the ferromagnet, yielding the same flow of minority and majority electrons through the FM layer in cw regime and thus leading to an overall vanishing spin photocurrent. This requirement of efficient recombination of minority electrons is usually not fulfilled in the hybrid FM/semiconductor devices investigated here. If negative or zero external bias is applied, there is no specific recombination channel for the electrons which have a spin-orientation opposite to the FM magnetization direction; in cw regime, this yields the same flow of electrons with spin-up and spin-down tunneling through the barrier and thus zero spin photocurrent can be measured.

However, if a competition channel (that allows recombination) exists, spin photocurrent might be measured. This could explain why some signature of spin photocurrent may have been evidenced for the devices of Ref. 31 under forward bias i.e., close to (but inferior to) the voltage corresponding to the flat-band situation. Nevertheless the interpretation of the experiments in the forward-bias regime is rather complicated since a large electron flow occurs simultaneously with the photocreated one.

In the end, let us comment a more recent experimental result evidenced on a hybrid device based on a GaAs quantum well and a Fe/Tb multilayer on top of an MgO tunnel barrier.[29] The novelty of this device is that the Fe/Tb multilayer structure exhibits spontaneous out-of-plane magnetization induced by interfacial magnetic anisotropy. Polarized photocurrent of about 3% was measured in this device for zero external magnetic field and the authors of this work demonstrated that this value is not due to the MCD in the FM layers. These results could thus be interpreted in terms of spin photocurrent due to the spin-filtering effect. However, the excitation conditions used in this work are very different to the ones used in previous work and in the present paper. The photocurrent was measured with an ultrafast laser (pulse width $\sim$80 fs) for the excitation source. This pulsed laser excitation has two consequences: the peak power is very large compared to the standard cw experiments (yielding a much larger photogenerated carrier density) and (ii) the photogenerated carriers are generated on a large spectral width ($\sim$25 meV). These two characteristics make the comparison

with the other experiments not straightforward. Though we cannot exclude the possibility of true spin photocurrent in this kind of device (the strong peak power might induced nonlinear effects yielding specific recombination channel for minority electrons in the semiconductor), we believe that further work is required to understand the exact role of the FM layer as a spin filter. Finally, because the problem of electron-hole recombination is involved, we believe that the remaining obstacles to the evidence of spin-polarized currents photogenerated in a seminconductor should be discriminated from those concerning all electrical injection-detection measurements.[15–21,46] More generally, the observation of spin-filtered photocurrents requires alternatives processes (other than the tunneling out process toward the ferromagnetic electrode), which are electron-hole recombination or reabsorption (by the source) processes as in giant magnetoresistance with metals. The general rule to obtain desired effect is to ensure a matching between the injection and detection impedances which is hardly attainable with standard spin-LEDs operated in reverse bias regime

In conclusion, we have demonstrated the fundamental differences between electrical spin injection and spin-polarized photocurrent detection in hybrid ferromagnetic-semiconductor devices. Though a very efficient electrical spin injection is demonstrated with a measured circular polarization of the electroluminescence up to 30% for an external field of 0.8 T, very weak polarizations of the photocurrent are evidenced whatever the device is. The maximum measured value of the photocurrent polarization obtained under resonant circularly polarized excitation of the quantum well excitons is about 3%. The investigated devices based on $AlGaAs/Al_2O_3/Co$ and AlGaAs/MgO/CoFeB layers do not act as efficient spin filters for the currents flowing from the semiconductor part to the ferromagnetic part of these structures though these layers are very efficient spin aligners for electrical spin injection. We interpret the weak measured polarization of the photocurrent as a consequence of the Zeeman splitting of the quantum well excitons which yields different absorption coefficients for the polarized excitation laser with different helicities. This leads to different photocurrent intensities measured for the two circularly polarized excitation cases. Finally, the requirement to measure large spin photocurrent due to the spin-filtering effect of the FM layer is the following: the minority photogenerated electrons which are reflected at the interface must be cancelled out through a channel competitive with the one corresponding to the back scattering from the semiconductor part toward the ferromagnetic layer. Engineering of new type of hybrid devices where this condition is fulfilled will be an important challenge in the future.

ACKNOWLEDGMENTS

We gratefully acknowledge A. Lemaître, P. Gallo, C. Fontaine, A. Arnoult, Y. Lu, M. Tran, R. Mattana, and C. Deranlot for the growth of the samples and D. Lagarde for her very efficient help during Photoluminescence Luminescence Excitation spectroscopy measurements. This work was partially supported by ANR INSPIRE. X. Marie thanks the support of Institut Universitaire de France (IUF). P. H. Binh thanks the support of Vietnam's National Foundation for Science and Technology Development (NAFOSTED) (code: 103.03.49.09).

[1] A. T. Hanbicki, O. M. J. van 't Erve, R. Magno, G. Kieseoglou, C. H. Li, B. T. Jonker, G. Itskos, R. Mallory, M. Yasar, and A. Petrou, Appl. Phys. Lett. **82**, 4092 (2003).
[2] P. Renucci, H. Jaffrès, J. M. George, T. Amand, and X. Marie, in *Spintronic Semiconductors*, edited by W. Chen and I. Buyanova (Pan Stanford, World Scientific, Singapore, 2010), Chap. 10.
[3] G. Aronov and G. E. Pikus, Fiz. Tekh. Poluprovodn. **10**, 1177 (1976) [Sov. Phys. Semicond. **10**, 698 (1976)].
[4] R. Fiederling, M. Keim, G. Reuscher, W. Ossau, G. Schmidt, A. Waag, and L. W. Molenkamp, Nature (London) **402**, 787 (1999).
[5] Y. Ohno, D. K. Young, B. Beschoten, F. Matsukura, H. Ohno, and D. D. Awschalom, Nature (London) **402**, 790 (1999).
[6] O. M. J. van 't Erve, G. Kioseoglou, A. T. Hanbicki, C. H. Li, B. T. Jonker, R. Mallory, and M. A. Petrou, Appl. Phys. Lett. **84**, 4334 (2004).
[7] G. Schmidt, D. Ferrand, L. W. Molenkamp, A. T. Filip, and B. J. van Wees, Phys. Rev. B **62**, R4790 (2000).
[8] A. Fert and H. Jaffrès, Phys. Rev. B **64**, 184420 (2001).
[9] A. Fert, J. M. George, H. Jaffrès, and R. Mattana, IEEE Trans. Electron Devices **54**, 921 (2007).
[10] X. Jiang, R. Wang, R. M. Shelby, R. M. Macfarlane, S. R. Bank, J. S. Harris, and S. S. P. Parkin, Phys. Rev. Lett. **94**, 056601 (2005).
[11] S. A. Crooker, M. Furis, X. Lou, C. Adelmann, D. L. Smith, C. J. Palmstrom, and P. A. Crowell, Science **309**, 2191 (2005).
[12] S. A. Crooker and D. L. Smith, Phys. Rev. Lett. **94**, 236601 (2005).
[13] J. Wunderlich, A. C. Irvine, J. Sinova, B. G. Park, L. P. Zârbo, X. L. Xu, B. Kaestner, V. Novák, and T. Jungwirth, Nat. Phys. **5**, 675 (2009).
[14] K. Ando, M. Morikawa, T. Trypiniotis, Y. Fujikawa, C. H. W. Barnes, and E. Saitoh, Appl. Phys. Lett. **96**, 082502 (2010).
[15] X. Lou, C. Adelmann, M. Furis, S. A. Crooker, C. J. Palmstrøm, and P. A. Crowell, Phys. Rev. Lett. **96**, 176603 (2006).
[16] X. Lou, C. Adelmann, S. A. Crooker, E. S. Garlid, J. Zhang, K. S. M. Reddy, S. D. Flexner, C. J. Palmstrøm, and P. A. Crowell, Nat. Phys. **3**, 197 (2007).
[17] D. Saha, M. Holub, and P. Bhattacharya, Appl. Phys. Lett. **91**, 072513 (2007).
[18] O. M. J. van 't Erve, A. T. Hanbicki, M. Holub, C. H. Li, C. Awo-Affouda, P. E. Thompson, and B. T. Jonker, Appl. Phys. Lett. **91**, 212109 (2007).
[19] M. Tran, H. Jaffres, C. Deranlot, J.-M. George, A. Fert, A. Miard, and A. Lemaitre, Phys. Rev. Lett. **102**, 036601 (2009).
[20] B. Huang, D. J. Monsma, and I. Appelbaum, Phys. Rev. Lett. **99**,

177209 (2007).
[21] S. P. Dash, S. Sharma, R. S. Patel, M. P. de Jong, and R. Jansen, Nature (London) **462**, 491 (2009).
[22] M. D'Yakonov, *Spin Physics in Semiconductors*, Springer Series in Solid-State Sciences Vol. 157 (Springer, Berlin, 2008), Chap. 3; F. Meier and B. Zakharchenya, *Optical Orientation*, Modern Problems in Condensed Matter Sciences Vol. 8 (North-Holland, Amsterdam, 1984).
[23] M. W. Prins, H. Van Kampen, H. Van Leuken, R. A. de Groot, W. Van Roy, and J. De Boeck, J. Phys.: Condens. Matter **7**, 9447 (1995).
[24] K. Nakajima, S. N. Okuno, and K. Inomata, Jpn. J. Appl. Phys., Part 2 **37**, L919 (1998).
[25] A. Hirohata, Y. B. Xu, C. M. Guertler, J. A. C. Bland, and S. N. Holmes, Phys. Rev. B **63**, 104425 (2001).
[26] A. F. Isakovic, D. M. Carr, J. Strand, B. D. Schultz, C. J. Palmstrom, and P. A. Crowell, Phys. Rev. B **64**, 161304(R) (2001).
[27] T. Manago, Y. Suzuki, and E. Tamura, J. Appl. Phys. **91**, 10130 (2002).
[28] T. Taniyama, G. Wastlbauer, A. Ionescu, M. Tselepi, and J. A. C. Bland, Phys. Rev. B **68**, 134430 (2003).
[29] S. Hövel, N. C. Gerhardt, M. R. Hofmann, F.-Y. Lo, D. Reuter, A. D. Wieck, E. Schuster, W. Keune, H. Wende, O. Petracic, and K. Westerholt, Appl. Phys. Lett. **92**, 242102 (2008).
[30] A. F. Isakovic, D. M. Carr, J. Strand, B. D. Schultz, C. J. Palmstrom, and P. A. Crowell, J. Appl. Phys. **91**, 7261 (2002).
[31] S. J. Steinmuller, C. M. Gürtler, G. Wastlbauer, and J. A. C. Bland, Phys. Rev. B **72**, 045301 (2005).
[32] Y. Lu, V. G. Truong, P. Renucci, M. Tran, H. Jaffrès, C. Deranlot, J.-M. George, A. Lemaître, Y. Zheng, D. Demaille, P.-H. Binh, T. Amand, and X. Marie, Appl. Phys. Lett. **93**, 152102 (2008).
[33] R. I. Dzhioev, K. V. Kavokin, V. L. Korenev, M. V. Lazarev, B. Ya. Meltser, M. N. Stepanova, B. P. Zakharchenya, D. Gammon, and D. S. Katzer, Phys. Rev. B **66**, 245204 (2002).
[34] Y. Lu, C. Deranlot, A. Vaurès, F. Petroff, J.-M. George, Y. Zheng, and D. Demaille, Appl. Phys. Lett. **91**, 222504 (2007).
[35] It is comparable with the definition of Refs. 26 and 30 where a modulation technique is employed.
[36] R. J. Soulen, Jr., J. M. Byers, M. S. Osofsky, B. Nadgorny, T. Ambrose, S. F. Cheng, P. R. Broussard, C. T. Tanaka, J. Nowak, J. S. Moodera, A. Barry, and J. M. D. Coey, Science **282**, 85 (1998).
[37] T. Amand, X. Marie, P. Le Jeune, M. Brousseau, D. Robart, J. Barrau, and R. Planel, Phys. Rev. Lett. **78**, 1355 (1997).
[38] B. Liu, M. Senès, S. Couderc, J.-F. Bobo, X. Marie, T. Amand, C. Fontaine, and A. Arnoult, Physica E **17**, 358 (2003).
[39] This relationship is a simplified version of the one of Ref. 38 because the rising time τ_r of luminescence is short compared to the polarization relaxation time τ_s. τ_r and τ_s (as well as τ) can be directly measured by TRPL (for example, at $T=20$ K, $\tau_r \approx 100$ ps, $\tau_s \approx 1000$ ps, so $\tau_r \ll \tau_s$).
[40] J. Barrau, G. Bacquet, F. Hassen, N. Lauret, T. Amand, and M. Brousseau, Superlattices Microstruct. **14**, 27 (1993).
[41] S. Pfalz, R. Winkler, T. Nowitzki, D. Reuter, A. D. Wieck, D. Hägele, and M. Oestreich, Phys. Rev. B **71**, 165305 (2005).
[42] Y. H. Chen, X. L. Ye, B. Xu, Z. G. Wang, and Z. Yang, Appl. Phys. Lett. **89**, 051903 (2006).
[43] M. J. Snelling, E. Blackwood, C. J. McDonagh, R. T. Harley, and C. T. B. Foxon, Phys. Rev. B **45**, 3922 (1992).
[44] O. Carmel, H. Shtrikman, and I. Bar-Joseph, Phys. Rev. B **48**, 1955 (1993).
[45] A. Hirohata, S. J. Steinmueller, W. S. Cho, Y. B. Xu, C. M. Guertler, G. Wastlbauer, J. A. C. Bland, and S. N. Holmes, Phys. Rev. B **66**, 035330 (2002).
[46] S. A. Crooker, E. S. Garlid, A. N. Chantis, D. L. Smith, K. S. M. Reddy, Q. O. Hu, T. Kondo, C. J. Palmstrom, and P. A. Crowell, Phys. Rev. B **80**, 041305(R) (2009).